Science
AAAS

Supplementary Materials for

Structure of a Janus Kinase cytokine receptor complex reveals the basis for dimeric activation

Authors: Caleb R. Glassman[1]†, Naotaka Tsutsumi[1,2]†, Robert A. Saxton[1,2], Patrick J. Lupardus[1]‡, Kevin M. Jude[1,2], K. Christopher Garcia[1,2,3*]

Affiliations:
[1]Department of Molecular and Cellular Physiology, Stanford University School of Medicine, Stanford, CA 94305, USA
[2]Howard Hughes Medical Institute, Stanford University School of Medicine, Stanford, CA 94305, USA
[3]Department of Structural Biology, Stanford University School of Medicine, Stanford, CA 94305, USA

*Corresponding author. Email: kcgarcia@stanford.edu
†Equal contribution
‡Present address: Synthekine, Menlo Park, CA 94025, USA

This PDF file includes:

Materials and Methods

Protein purification

To mimic cytokine receptor dimerization, a construct consisting of N-terminal glutathione S-transferase followed by a 9 amino acid linker (SDGSTSGSG), 3C protease site, GCN4 leucine zipper, and *Mus musculus* interferon lambda receptor 1 (IFNλR1) Box1/Box2 (mIFNlR1 249-298), which we refer to as mini-IFNλR1, was cloned into a modified pAc vector for baculoviral expression. For JAK expression, full-length *Mus musculus* Janus Kinase 1 (mJAK1 1-1153) with C-terminal BC2 (DRKAAVSHWQ) and 8xHis tags was cloned into pAc with or without activating V657F mutation.

To stabilize the complex, tandem BC2 nanobodies (*37)* separated by a 5 amino acid linker (GSRGS) were cloned into pD649 vector with N-terminal signal peptide and C-terminal AviTag and 6xHis tag (BiBC2 nanobody). Protein was expressed by transient transfection of Expi293F cells (Gibco) using ExpiFectamine 293 Transfection Kit (Gibco) according to manufacturer's protocols. Supernatants were subject to Ni-NTA purification and Size Exclusion Chromatography (SEC) using Superdex 75 10/300 GL column (Cytiva).

Spodoptera frugiperda (*Sf9*) ovarian cells (ATCC) were maintained in Sf-900 III medium (Gibco) with 10% (v/v) FBS (Sigma) and GlutaMAX (Gibco) and baculovirus was produced by transfection with FuGENE HD (Promega) and BestBac 1.0 Linearized Baculovirus DNA (Expression Systems) followed by viral amplification in Sf9. Protein was expressed in *Trichoplusia ni* (*T. ni*) ovarian cells (Expression Systems) maintained in ESF 921 Insect Cell Culture Medium (Expression Systems) at 27°C with ambient CO_2 and gentle agitation. *T. ni* cells were coinfected with mini-IFNλR1 and mJAK1 baculovirus for 48 hours. Cells were washed once in Phosphate Buffered Saline (PBS) pH7.4 and resuspended in a lysis buffer of 50 mM Tris-HCl

pH 8.5, 0.5 M NaCl, 1 mM adenosine (Sigma), 1 mM TCEP, and 10% (v/v) glycerol supplemented with 15 mM imidazole, protease inhibitor cocktail (Sigma), and benzonase (Sigma). Cells were lysed by Dounce homogenization followed by ultracentrifugation and the soluble fraction was subject to affinity purification using High Affinity Ni-Charged Resin (GenScript) in the presence of 0.005% (w/v) n-dodecyl β-D-maltoside (DDM). Nickle resin was washed with lysis buffer supplemented with 30 mM imidazole and 0.005% (w/v) DDM prior to elution with increased imidazole concentration to 250 mM. To capture mJAK1-IFNλR1 complex, the elution was incubated with Glutathione Sepharose 4 Fast Flow Resin (Cytoiva) prior to washing in buffer composed of 20 mM HEPES-Na pH 8.0, 0.5 M NaCl, 1 mM adenosine, 1mM TCEP, 10% (v/v) glycerol, and 0.005% (w/v) DDM. GST-tagged protein was eluted in wash buffer supplemented 20 mM reduced glutathione and adjusted to pH 7.4. Glutathione elution was concentrated and buffer exchanged in glutathione wash buffer prior to complexing with stoichiometric BiBC2 nanobody and cleaving with 1:10 (w/w) 3C protease for 1 hour at room temperature. Superose 6 (Cytiva) SEC was used to separate mJAK1-IFNλR1 complex from free GST in a buffer consisting of 20 mM HEPES-Na pH 8.0, 0.5 M NaCl, 1 mM adenosine, 1% (v/v) glycerol, and 1 mM TCEP. Fractions containing complex were passed over a glutathione column to remove any residual un-cleaved protein and free GST. Purified sample was crosslinked with 1 mM bis(sulfosuccinimidyl)suberate (BS3) (Thermo) for 30 min at room temperature and quenched with 20 mM Tris-HCl pH 8. The cross-linked complex was buffer-exchanged to 20 mM HEPES-Na pH 8, 0.5 M NaCl, 1 mM adenosine, 1% (v/v) glycerol, and 1 mM TCEP on a Vivaspin 500 centrifugal concentrators (Satorius, 100,000 MWCO) and concentrated to 6 mg/ml for cryo-EM experiments.

Cryo-EM sample preparation, data collection, processing, and 3D reconstruction

To prepare the cryo-EM specimens, cross-linked complex was supplemented with 0.005% DDM immediately before freezing. 3.0 μL of sample was applied to a glow-discharged 300 mesh gold grid (Quantifoil R1.2/1.3) and excess sample was blotted to a filter paper for 3 sec before plunge-freezing using a Leica EM GP (Leica Microsystems) at 20°C and 95% humidity. Cryo-EM movies were collected using an FEI Titan Krios operated at 300 kV equipped with Gatan K3 camera in counting mode. Nominal magnification was set to 29,000x, corresponding to a calibrated magnification of 58,680x and a super-resolution pixel size of 0.42605 Å. Movies were recorded using SerialEM (*62)* for 2.5 sec with 0.05 sec exposure per frame at an exposure rate of ~16 electrons/pixel/sec at the specimen, and the defocus range between -1.0 and -2.0 μm. A beam-image shift was used with an active calibration to collect 18 movies from 9 holes per stage shift and autofocus.

Collected movies were processed and assessed with cryoSPARC Live. Patch motion correction was performed with binning to a pixel size of 0.8521 Å, and patch contrast transfer function (CTF) parameters were estimated with a default setting. Curated 29,467 movies were used for the downstream processing with cryoSPARC *(63)*. Particles were picked with 2D templates from preliminary experiments and extracted with a box size of 400 pixels, binned to 64 pixels. Multiple rounds of 2D classifications were used to remove extracted buffer features and contaminants, yielding 1,429,325 particles that appeared to be protein. After re-extracting particles with the 400/256 binned box, further 2D classifications, a 2-class ab-initio reconstruction followed by two rounds of heterogeneous refinements generated 589,565-particle set for an initial non-uniform refinement *(64)*. At this stage, we were able to locate individual domains and the "nanobody clump" in the consensus refined map (**Fig. S2**). 3-component 3D variability analysis *(65)* was performed for this aligned particle set which allowed us to identify two classes for further

heterogeneous refinement: 1 - a class with the clearer FERM-SH2 dimer and one of the nanobodies poorly visualized, and 2 - a class with the partially broken FERM-SH2 dimer and the better defined nanobody dimer. The former class could be refined with C2 symmetry which resulted in a JAK1-IFNλR1 dimer and blurred nanobody densities. A C2 symmetry-imposed *ab-initio* 3D reconstruction, heterogeneous refinements, a non-uniform refinement, and CTF refinements (per-group tilt and anisotropic magnification, and per-particle CTFs) followed by a non-uniform refinement yielded a 4.0 Å nominal resolution map with 224,615 particles as determined by gold-standard Fourier shell correlation (FSC) using the 0.143 criterion. The final map was generated with a local non-uniform refinement with a mask covering the whole mIFNλ-mJak1 complex but excluding the nanobodies, which yielded 3.6 Å nominal resolution map. Focused classifications and refinements with C2 symmetry expansion and various local masks did not generate a better particle set or a 3D reconstruction based on visual inspections of the maps. The final map was sharpened with the full map-based deepEMhancer *(66)* for model building and overall map representation, and the half map-based Phenix *(67)* local anisotropic sharpening for model building, visualization of local maps overlaid on the structural model, and real-space refinement.

Model building and refinement

The crystal structures of human JAK1 FERM-SH2 (PDB ID: 5IXD), PK (4L00), and TK (3EYG) were docked into the 3D reconstructions using UCSF ChimeraX *(68)* for an initial interpretation of the maps *(14,39,40)*. A homology model of full-length mouse JAK1 was then created using the docked model on the SWISS-MODEL server (swissmodel.expasy.org). The SH2 domain was replaced with the AlphaFold2 model *(69)*, and the overall structure was fitted into the cryo-EM map with segmental rigid-body fits on Coot *(70)*. The model was corrected and refined iteratively

using Coot for manual building, ISOLDE *(71)* on ChimeraX to improve the geometry and secondary structures, and Phenix for real-space refinement. We used the unsharpened map, deepEMhanceer sharpened map, and Phenix local anisotropic sharpened map for modeling. The structure and map were visualized using UCSF ChimeraX. All secondary structures in the figures were assigned using DSSP. Shape complementarity statistic were quantified using SC implemented in CCP4 *(72)*. The map counter levels are indicated either in figure captions or panels when appropriate. The buried surface area was calculated using PDBePISA (www.ebi.ac.uk/pdbe/pisa) *(73)*. Active-state human JAK2 Val^{617}→Phe model was generated with the SWISS-MODEL server using the full JAK2 sequence, and the current structure as a template.

Cell signaling assays

To assess the ability of mini-IFNλR1 to activate JAK1, we infected *T. ni* cells with baculovirus encoding mJAK1 (wild-type or V657F) and mini-IFNλR1. After 48 hours of infection, cells were harvested, washed once in ice-cold PBS, and lysed in PBS supplemented with 1% (w/v) DDM and one tablet of cOmplete protease inhibitor cocktail (Roche) per 10 mL lysis buffer. Lysates were resolved on 12% SDS-PAGE (BioRad) and transferred to PVDF membranes using Trans-Blot Turbo Transfer System (BioRad). Membranes were blocked for 1 hour in TBS-T (20 mM Tris-HCl pH7.4, 150 mM NaCl, 0.1% (v/v) Tween 20) containing Blotting-Grade Blocker (BioRad). Primary antibodies against phosphoTyr1034-1035 JAK1 (Cell Signaling Technology clone 3331) and total JAK1 (Cell Signaling Technologies clone 6G4) were detected with swine anti-rabbit HRP (Dako) and enhanced chemiluminescence (ECL) detection reagent (Cytiva). Blots were developed on Hyperfilm ECL (Cytiva).

For mammalian cell signaling experiments, mouse erythropoietin receptor (mEpoR 25-507) was cloned into pLV lentiviral vector with N-terminal HA signal peptide and HA tag. To generate the mEpoR-IFNλR1 Box1/Box2 chimera, the Box1/Box2 region of EpoR (273-338) was replaced with that of IFNλR1 (249-298). NIH 3T3 mouse fibroblasts were maintained in Dulbecco's Modified Eagle Medium (DMEM, Gibco), supplemented with 10% FBS (Sigma) and 2 mM GlutaMAX (Gibco). Receptor constructs were transiently transfected into NIH 3T3 cells using FuGene HD transfection reagent (Promega). 48 hours post transfection, cells were stimulated for 20 min with 10 ng/mL mouse erythropoietin (Epo, R&D systems). Cells were rinsed once with ice-cold PBS and lysed with Triton lysis buffer (1% (v/v) Triton X-100, 20 mM HEPES-Na pH 7.4, 150 mM NaCl) supplemented with one tablet of PhosSTOP phosphatase inhibitor cocktail (Roche), and one tablet of EDTA-free cOmplete protease inhibitor cocktail (Roche) per 10 ml of buffer. The cell lysates were cleared by centrifugation at 15,000g at 4°C for 10 min. Cell lysates were denatured by the addition of SDS sample buffer and boiling for 5 min, resolved by SDS-PAGE, and analyzed by immunoblotting as described above with the addition of primary antibodies against phospho-Tyr1007 JAK2 (Cell Signaling Technologies clone D15E2), phospho-Tyr1034/1035 JAK1 (Cell Signaling Technologies clone 3331), total JAK2 (Cell Signaling Technologies clone D2E12), and total JAK1 (Cell signaling technologies clone 6G4).

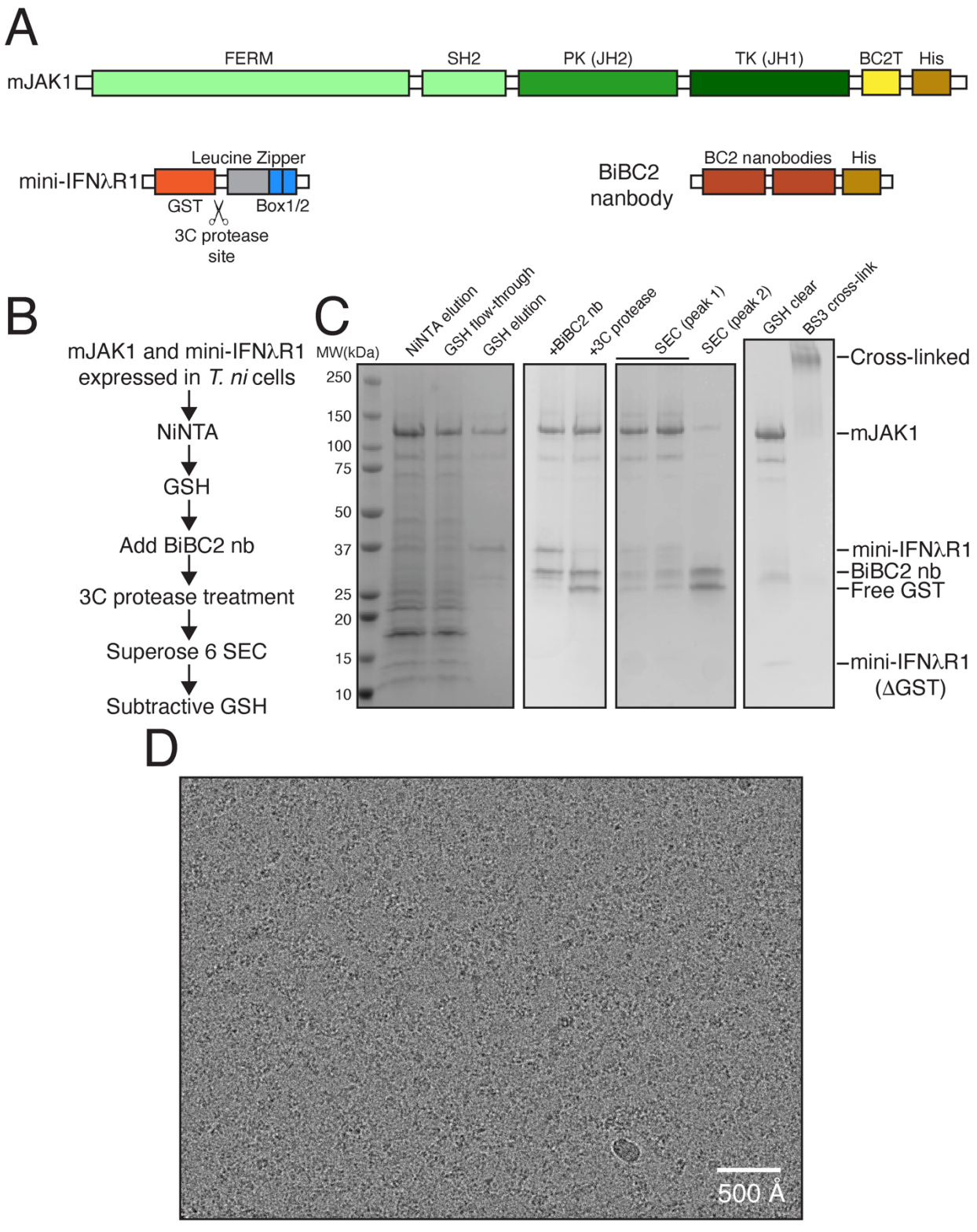

Fig. S1. Purification and cryo-EM imaging of an active JAK1-IFNλR1 complex.

(**A**) Linear schematic of the JAK1-IFNλR1 complex. The complex is held together at the top by homodimeric leucine zippers fused to Box1/Box2 of IFNλR1 which engage the FERM-SH2 domains of mJAK1 and at the bottom by a tandem BC2 nanobody (BiBC2) which engages an BC2 tag (BC2T) at the C-terminus of mJAK1. (**B**) Overview of the two-step affinity purification scheme to capture active JAK1-IFNλR1 complex. (**C**) SDS-PAGE of the purification process. Samples were run on a 4-20% gradient gel and visualized using colloidal blue staining. (**D**) Representative micrograph from cryo-EM data collection.

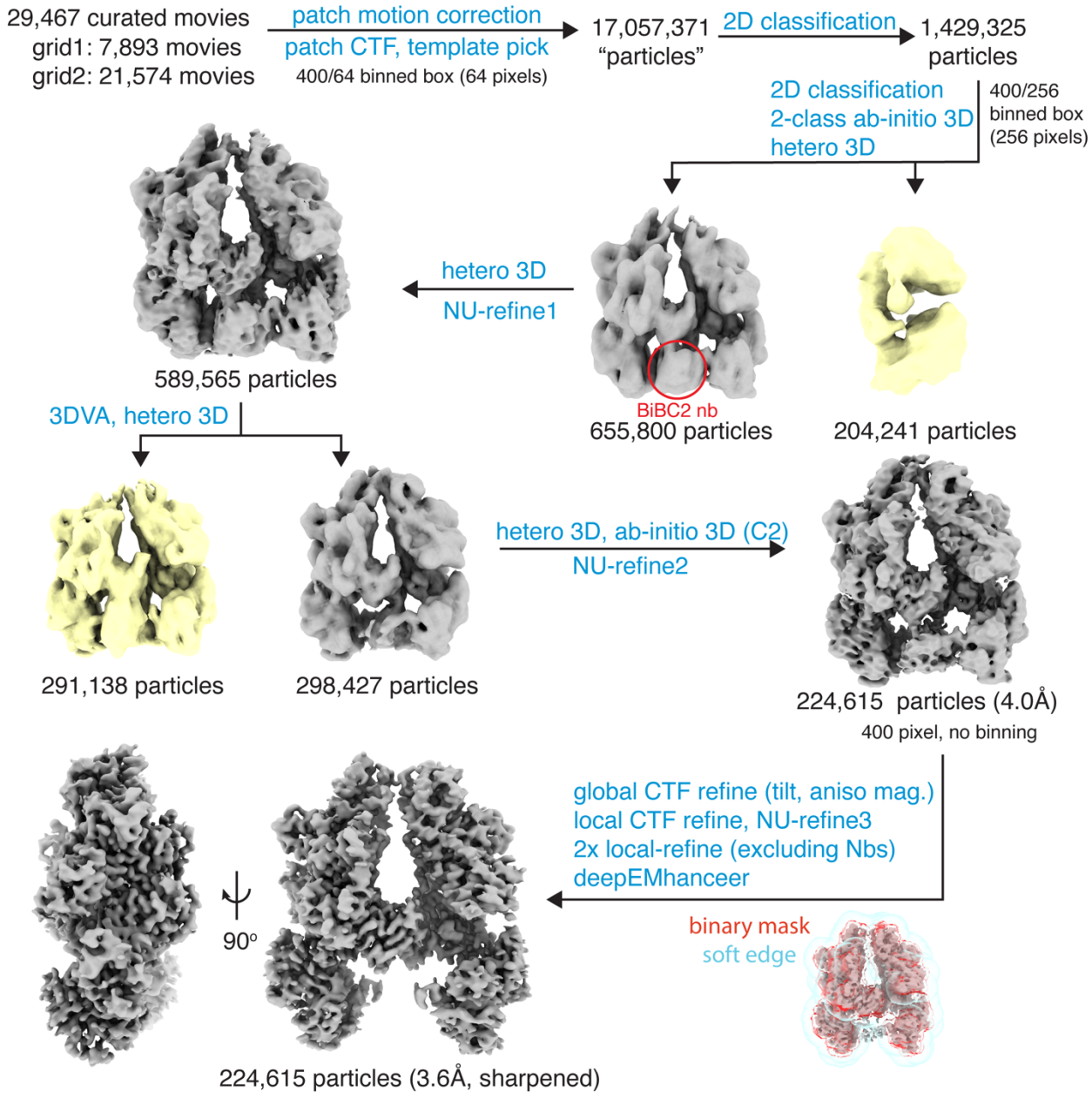

Fig. S2. Cryo-EM data processing scheme. Cryo-EM data analysis workflow is shown with representative 3D reconstructions during the data processing. BiBC2 nanobody is indicated by the red circle in the figure where first observed in the cryo-EM density. Template pick: template-based particle picking and extraction, ab-initio 3D: ab-initio 3D reconstruction, hetero 3D: heterogeneous 3D refinement, NU-refine: non-uniform refinement, 3DVA: 3D variability analysis, local-refine:

non-uniform local refinement with the mask indicated at the right bottom (red: binary mask, blue: soft mask edge).

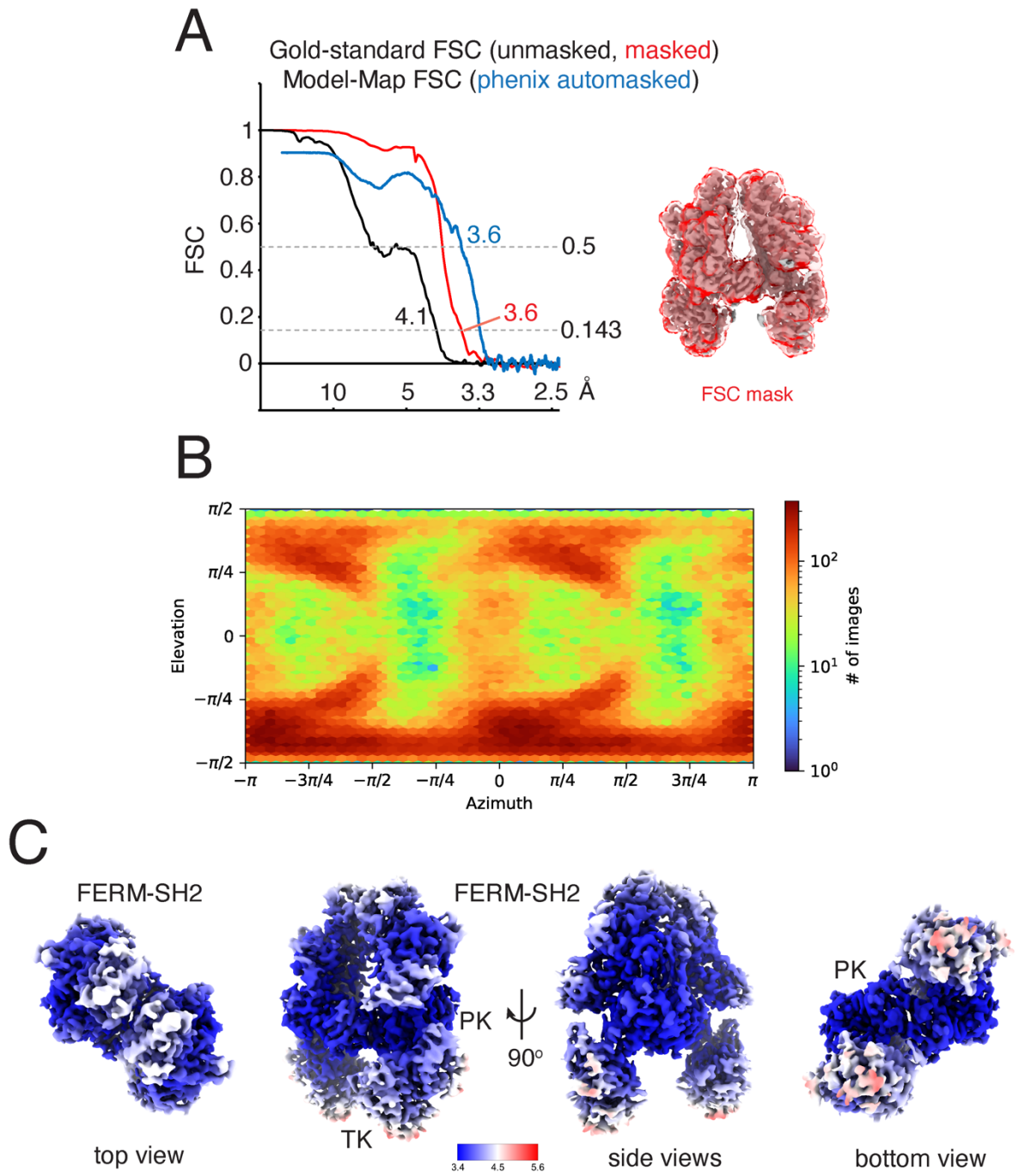

Fig. S3. Cryo-EM data assessment. (**A**) Gold-standard FSC curves with (black) or without (red) the FSC mask shown on the right as semi-transparent surface (red) overlaid on the deepEMhancer sharpened map (gray), and model-map FSC curve (blue). The gold-standard FSC was calculated

using cryoSPARC, and the model-map FSC was made with Phenix. (**B**) Orientation distribution of the alignment particles in the final 3D reconstruction output from cryoSPARC. (**C**) Local resolution estimates by Phenix color on the surface representation of the deepEMhancer sharpened map. The blue-white-red gradient corresponds to 3.4, 4.5, and 5.6 Å resolution, respectively.

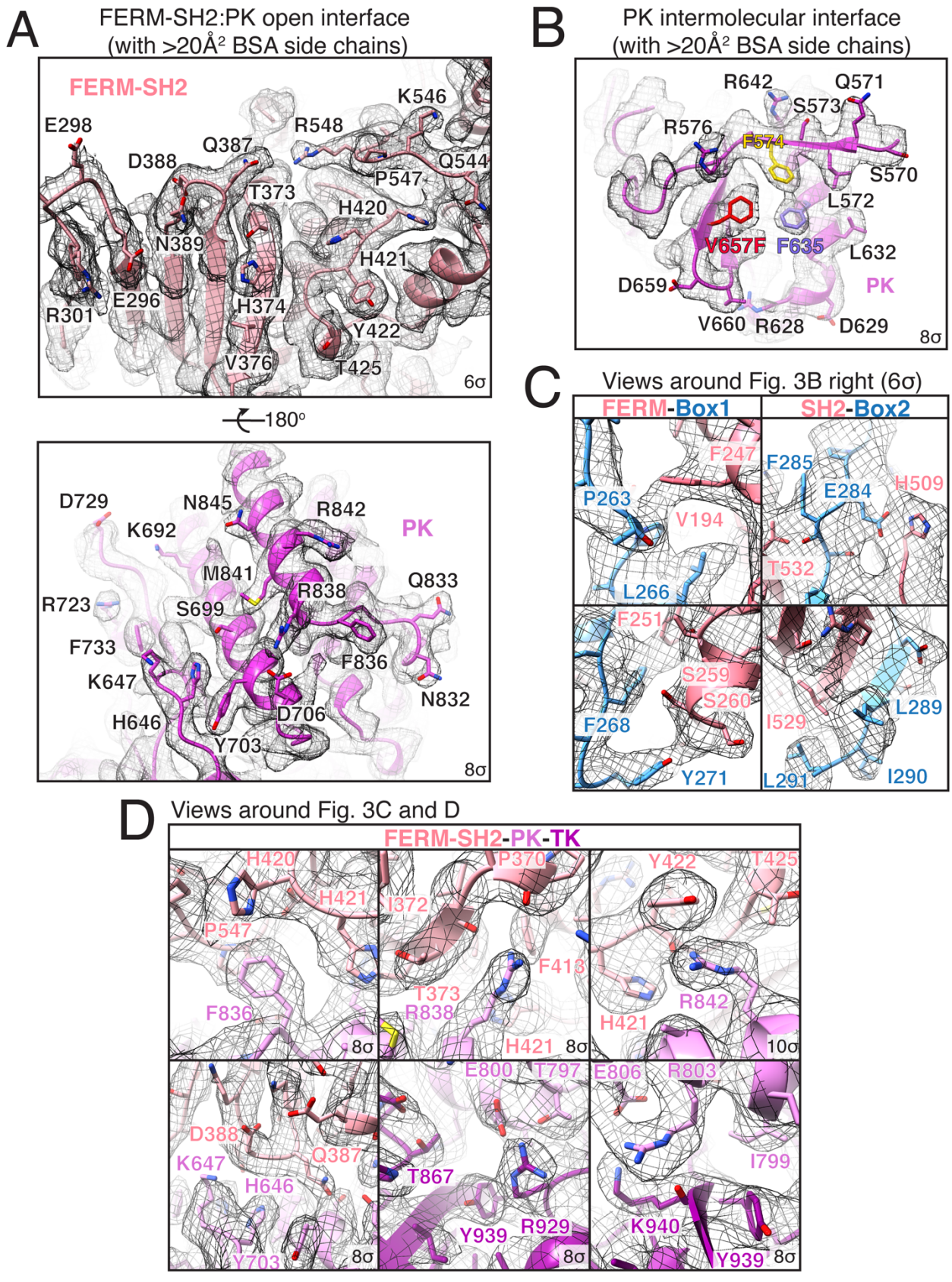
A
FERM-SH2:PK open interface
(with >20Å² BSA side chains)
FERM-SH2
E298
D388
Q387
R548
K546
Q544
P547
T373
H420
N389
H421
E296
R301
H374
Y422
V376
T425
6σ
180°
D729
N845
R842
K692
PK
M841
Q833
R838
R723
S699
F733
F836
K647
N832
D706
H646
Y703
8σ
B
PK intermolecular interface
(with >20Å² BSA side chains)
R642
Q571
S573
R576
F574
S570
L572
V657F
F635
L632
D659
PK
V660
R628
D629
8σ
C
Views around Fig. 3B right (6σ)
FERM-Box1
SH2-Box2
F247
F285
H509
P263
E284
V194
T532
L266
F251
S259
S260
F268
I529
L289
Y271
L291
I290
D
Views around Fig. 3C and D
FERM-SH2-PK-TK
H420
H421
P547
F836
8σ
P370
I372
F413
T373
R838
H421
8σ
Y422
T425
R842
H421
10σ
D388
K647
Q387
H646
Y703
8σ
E800
T797
T867
Y939
R929
8σ
E806
R803
I799
K940
Y939
8σ

Fig. S4. Representative cryo-EM density at the interfaces. (**A**) The open interface of the intramolecular FERM-SH2:PK packing in a mJAK1 monomer unit. The cryo-EM map (black) is overlaid on the ribbon models of FERM-SH2 (top, pink) and PK (bottom, orchid). (**B**) The mJAK1 intermolecular PK-PK interface. The cryo-EM map (black) is overlaid on the ribbon models of PK (orchid). The amino acid residues contributing to the interface formation with >20Å^2 buried surface area (BSA) are shown as sticks. Phenylalanine side chains are colored in gold (Phe^{574}), slate blue (Phe^{635}) and red (Phe^{657}). (**C**) Cryo-EM density depicted around the IFNλR1 Box1-mJAK1 FERM (top) and IFNλR1 Box2-mJAK1 SH2 (bottom) interfaces, corresponding to the region around the main figure 3B right. (**D**) Cryo-EM density for the mJAK1 intramolecular packing, corresponding to the region around the main figure 3C and D. The map counter levels are indicated in the figure panels.

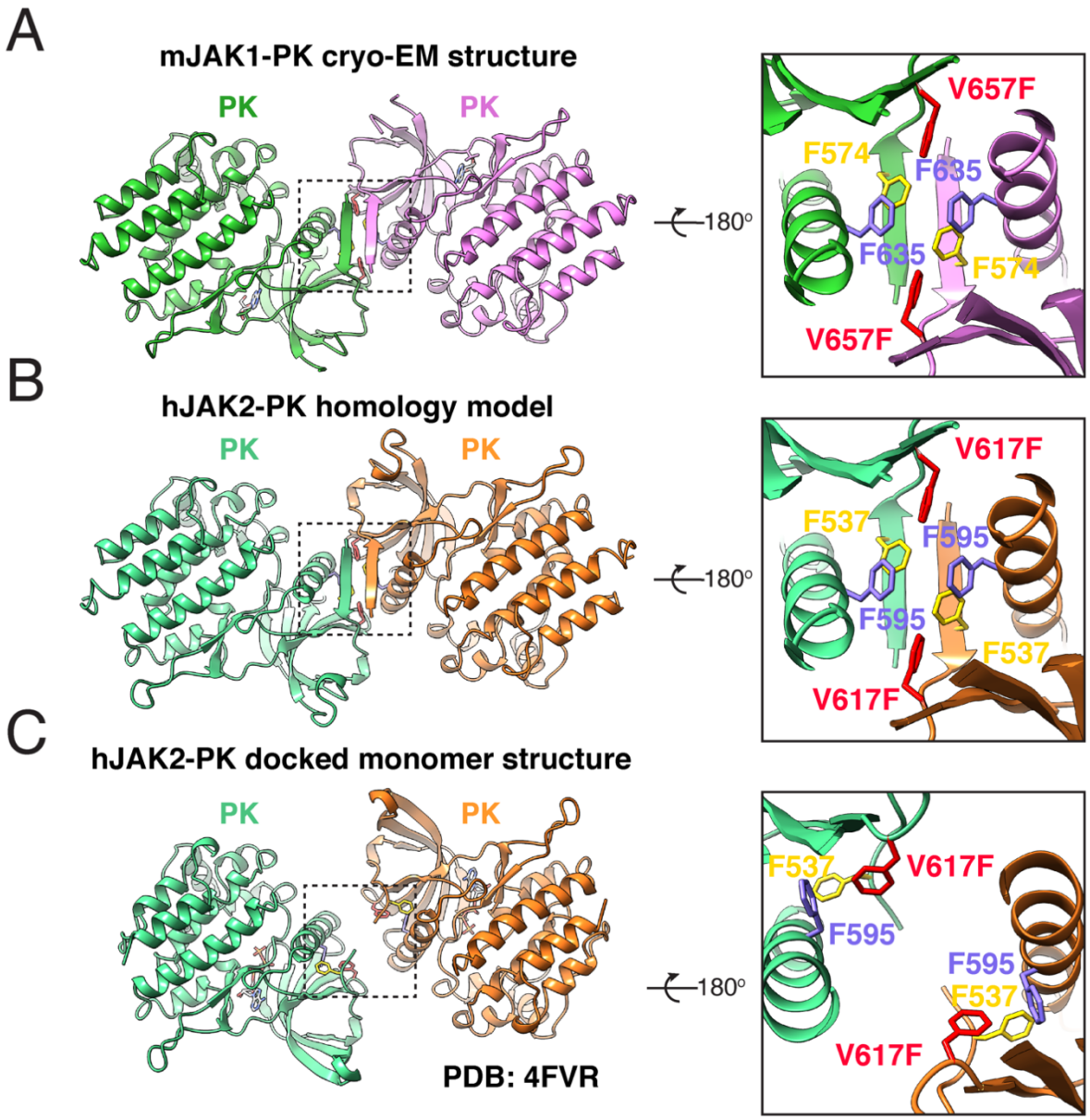

Fig. S5. Homology model of the active hJAK2 PK homodimer. (**A**) Cryo-EM structure of the 2:2 JAK1-IFNλR1 Val→Phe PK dimer as viewed from the top (left) and bottom (right). PK domains are colored in green and orchid, phenylalanine side chains are colored in gold (Phe^{574}), slate blue (Phe^{635}) and red (Phe^{657}). (**B**) Homology model of the hJAK2 Val→Phe dimer generated with the SWISS-MODEL server based on the cryo-EM structure of the mJAK1-IFNλR1 dimer.

The JAK2 homology model shows similar PK dimerization observed in the JAK1 complex with the anti-parallel β-sheet and phenylalanine cluster. JAK2 PK domains are colored green and orange. Phenylalanine triad is colored as follows: gold (Phe^{537}), slate blue (Phe^{595}) and red (Phe^{617}) (**C**) Monomeric hJAK2 PK Val→Phe crystal structure (PDB ID: 4FVR) aligned to the JAK1-IFNλR1 cryo-EM structure reported here. Monomer structure shows movement of Phe^{595} and Phe^{617} side chains relative to their position within the active JAK1-IFNλR1 dimer. Phe^{537} in the SH2-PK linker is rotated outwards placing the aromatic ring away from the dimerization interface observed in the JAK1-IFNλR1 structure.

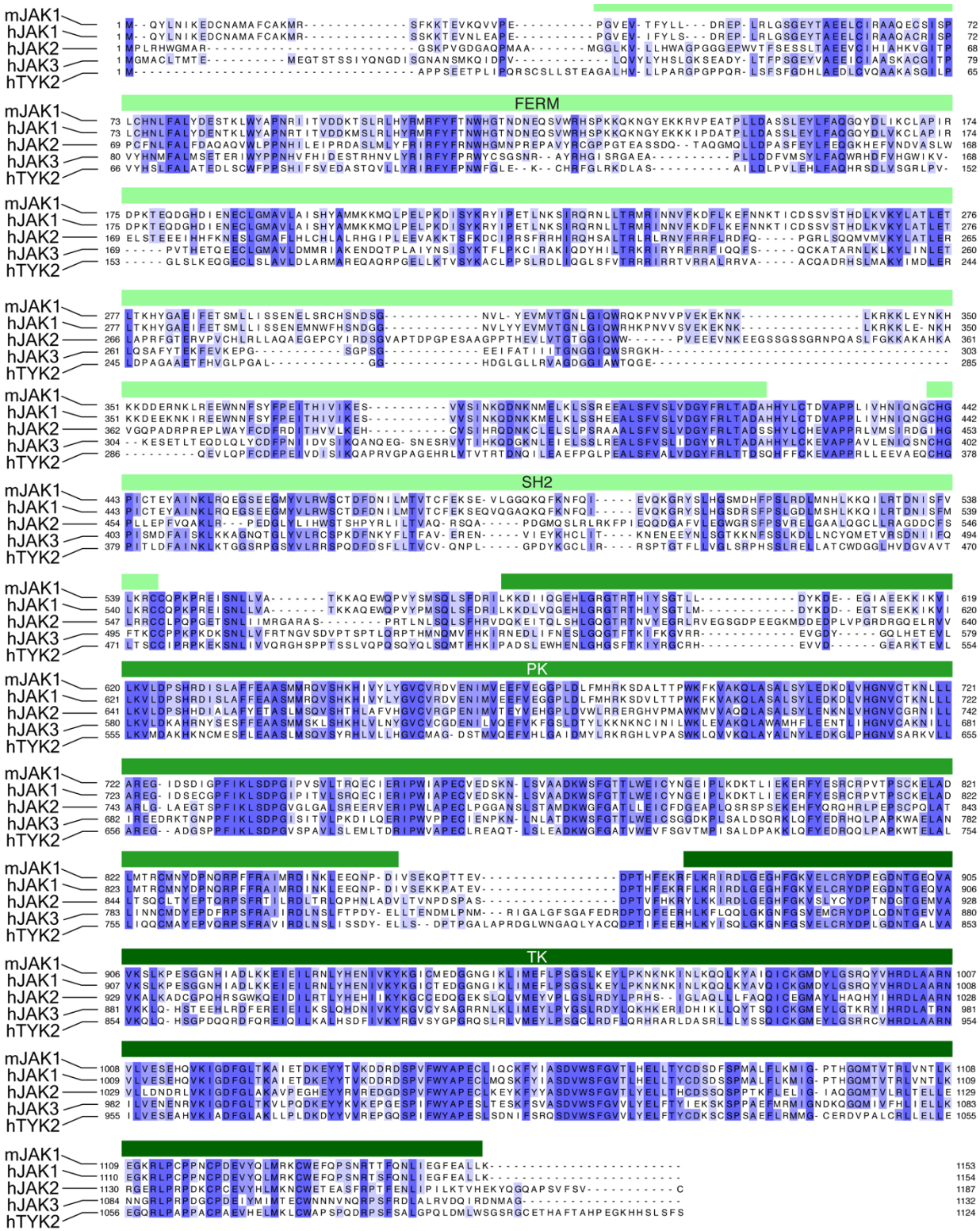
mJAK1
hJAK1
hJAK2
hJAK3
hTYK2
FERM
SH2
PK
TK

Fig. S6. Sequence alignment of Janus Kinase family members. Amino acid sequences of mouse JAK1, human JAK1, human JAK2, human JAK3, and human TYK2 were aligned using MAFFT version 7 (www.mafft.cbrc.jp/alignment/server/) and colored according to percentage identity using Jalview 2.11.17.

	mIFN-λ-mJak1 V657F homodimer (EMDB-25715, PDB 7T6F)
Data collection and processing	
Nominal magnification	29,000x
Calibrated magnification	58,680x
Voltage (kV)	300
Electron exposure (e/Å^2)	55
Defocus range (μm)	-1.0 to -2.0
Pixel size (Å)	0.8521
Symmetry imposed	C2
Initial "particle" images (no.)	17,057,371
Protein particle images (no.)	1,429,325
Final particle images (no.)	224,615
Map resolution (Å)	3.6
FSC threshold	0.143
Map resolution range (Å)	3.4 to 5.6
Refinement	
Initial model used (PDB code/AF2 code*)	5IXD, 4L00, 3EYG/AF-P52332-F1
Model resolution (Å)	3.6
FSC threshold	0.5
Map sharpening method	deepEMhanceer (visualization) Phenix LocalAniso (refinement&visualization)**
Model composition	
Non-hydrogen atoms	17,062
Protein residues	2,164
Ligands	4 (2 ADN and 2 ADP)
B factors (Å^2)	
Protein	106.58
Ligand	98.51
R.m.s. deviations	
Bond lengths (Å)	0.003
Bond angles (°)	0.548
Validation	
MolProbity score	1.74
Clashscore	4.82
Poor rotamers (%)	2.22
Ramachandran plot	
Favored (%)	96.53
Allowed (%)	3.47
Disallowed (%)	0
EMRinger score	2.35

*AlphaFold2 model. **Phenix local anisotropic sharpening based on half maps.

Table S1. Cryo-EM data collection and refinement statistics.

	V657F (PDB: 7T6F)	F657->V657 model	F657/V657
Interface	SC		SC ratio (%)
PK:PK	0.530	0.510	104
Residues	BSA (Å^2)		BSA ratio (%)
Met569	11.9	11.9	100
Ser570	57.1	57.1	100
Gln571	44.4	44.3	100
Leu572	71.5	67.4	106
Ser573	27.3	27.2	100
Phe574	62.8	68.1	92
Asp575	18.7	18.7	100
Arg576	116.8	123.1	95
Arg628	21.4	21.4	100
Asp629	39.2	39.2	100
Leu632	66.5	69.8	95
Phe635	40.3	38.7	104
Glu636	18.2	18.2	100
Arg642	28.0	28.0	100
Phe/Val657	**67.3**	**54.8**	**123**
Asp659	35.1	35.0	100
Val660	30.7	30.7	100

Table S2. Shape complementarity statistic (SC) and residue-by-residue buried surface area (BSA) at the mJAK1 intermolecular PK:PK interface. BSAs were calculated using the PDBe-PISA server (www.ebi.ac.uk/pdbe/pisa/), and amino acid residues with >10Å^2 BSA are listed. Sc values were quantified using CCP4 SC.

REAGENT or RESOURCE	SOURCE	IDENTIFIER
Antibodies		
JAK1 (6G4) Rabbit mAb	Cell Signaling Technologies	Cat#3344S
Phospho-Jak1 (Tyr1034/1035) Antibody	Cell Signaling Technologies	Cat#3331
Jak2 (D2E12) Rabbit mAb	Cell Signaling Technologies	Cat#3230S
Phospho-Jak2 (Tyr1007) (D15E2) Rabbit mAb	Cell Signaling Technologies	Cat#4406
Anti-rabbit Ig HRP	Dako	Cat#P0399
Cell Lines		
Expi293F	Gibco	Cat#A14527
Spodoptera frugiperda (*Sf9*)	ATCC	Cat#CRL-1711
Trichoplusia ni (*T. ni*)	Expression Systems	Cat#94-002F
NIH 3T3	ATCC	Cat#CRL-1658
Chemicals and commercial reagents		
Cellfectin II	Gibco	Cat#10362100
ExpiFectamine 293 Transfection Kit	Gibco	Cat#A14525
BestBac 1.0 Linearized Baculovirus DNA	Expression systems	Cat#91-001
FuGene HD transfection reagent	Promega	Cat#E2312
Expi293 Expression Medium	Gibco	Cat#A1435101
Sf-900 III Media	Invitrogen	Cat#12658019
ESF 921 Insect Cell Culture Medium	Expression Systems	Cat#96-001-01
Dulbecco's Modified Eagle Medium (DMEM), high glucose, no glutamine	Gibco	Cat#11960044
Fetal Bovine Serum (FBS)	Sigma-Aldrich	Cat#F7524
cOmplete protease inhibitor cocktail	Roche	Cat#11697498001
Protease Inhibitor Cocktail	Sigma-Aldrich	Cat#P8849
Phosphate-buffered saline (PBS), pH 7.2	Gibco	Cat#20012027
Blotting-Grade Blocker	BioRad	Cat#1706404
GlutaMAX	Gibco	Cat#35050061
12% Mini-PROTEAN TGX Precast Protein Gels	BioRad	Cat#4561046
Trans-Blot Turbo RTA Mini 0.2μm PVDF Transfer Kit	BioRad	Cat#1704272
ECL Prime Western Blotting Detection Reagent	Cytiva	Cat#45002401
Hyperfilm ECL	Cytiva	Cat#28906839
Mouse erythropoietin (Epo)	R&D systems	Cat#959-ME-010/CF
PhosSTOP	Roche	Cat#4906845001
High Affinity Ni-Charged Resin	GenScript	Cat#L00223
Glutathione Sepharose 4 Fast Flow	Cytiva	Cat#17513201
Superose 6 Increase 10/300 GL	Cytiva	Cat#29091596
Superdex 75 10/300 GL	Cytiva	Cat#29148721
n-Dodecyl β-D-maltoside (DDM), Sol-Grade	Anatrace	Cat#D310S
Tween 20	Sigma-Aldrich	Cat#P1379
Triton X-100	Sigma-Aldrich	Cat#X100
Tris Hydrochloride (Tris-HCl)	Fisher Scientific	Cat#BP153
Tris-Base	Fisher Scientific	Cat#BP152
HEPES	Fisher Scientific	Cat#BP310
Imidazole	ACROS Organics	Cat#122025000

Sodium Chloride	Fisher Scientific	Cat#S271
Benzonase Nuclease	Sigma-Aldrich	Cat#E1014
Vivaspin 500, 100,000 MWCO	Satorius	Cat#VS0142
L-Glutathione reduced (GSH)	Sigma-Aldrich	Cat#G4251
Tris(2-carboxyethyl)phosphine (TCEP)	Thermo Scientific	Cat#77720
Adenosine	Sigma-Aldrich	Cat#A9251
Glycerol	Fisher Scientific	Cat#BP229
BS3 (bis(sulfosuccinimidyl)suberate)	Thermo Scientific	Cat#21580
Quantifoil R1.2/1.3 Holey Carbon Grids, 300 Mesh Gold	Quantifoil	Cat#4230G

Table S3. Cell lines and reagents used in this study.